Chemical and Process Engineering 2013, 34 (3), 347-359
DOI: 10.2478/cpe-2013-0028

NUMERICAL GENERATION OF A FIXED BED STRUCTURE

Maciej Marek

Częstochowa University of Technology, Institute of Thermal Machinery, al. Armii Krajowej 21, 42-200 Częstochowa, Poland

A numerical algorithm is presented for the filling process of a cylindrical column with equilateral cylinders. The process is based on simplified mechanics – the elements are added one by one until the mechanical equilibrium is reached. The final structure is examined with respect to the global and local porosity distribution. Oscillating radial porosity profile is obtained in accordance with experimental data.

Keywords: fixed bed, porosity, structure, numerical modelling

1. INTRODUCTION

Fixed beds as a dense structure of randomly oriented elements within a cylindrical container (column) are widely employed in chemical engineering to increase contact surface of two or more reacting substances e.g. in absorber column of a carbon dioxide capture systems in CCS installations. Geometrical properties of the structure, such as porosity and its distribution on the cross-section of the bed, are crucial for the efficiency of the heat and mass transfer in the considered chemical process. The problem of porosity estimation has been extensively studied in the literature both from numerical and experimental point of view. Advantages of numerical analysis include its lower cost, full control over the process and unrestricted access to the structure parameters. Still, experiments are necessary for the validation of models and assessment of their limitations.

Numerical generation of dense random structure is, of course, considerably more challenging than the case of structured packing in which the position and orientation of a given element is strictly defined. In random structures, when an element can have arbitrary orientation, a special algorithm is needed to pack elements closely and prevent them from overlapping. The collision (contact) detection is particularly straightforward in the case of spherical elements (determination of the distance between their centers is sufficient) and majority of the work in this area concerns such elements (Mueller, 1992, 2005; Ritvanen and Jalali, 2008; Salvat et al., 2005; Siiria and Yliruusi, 2007; Theuerkauf et al., 2006) or similar shapes that can be easily handled, like spherocylinders (Abreu et al., 2003). General elements are typically approximated by a composition of spheres (Nolan and Kavanagh, 2005; Roskilly et al., 2010; Zhao et al., 2011), pixels (Caulkin et al., 2009; Jia and Williams, 2001) or by triangulation (Nandakumar et al., 1999). Even for cylindrical elements the contact detection is highly non-trivial and direct geometrical treatment is rather rare in the literature (Kodam et al., 2012; Guo et al, 2012).

Different approaches have been taken for bed generation. Some of them employ Discrete Element Method (DEM) simulations with complete or simplified mechanics of the process (Matuttis et al., 2000; Siiria and Yliruusi, 2007), other - Monte Carlo simulations in which initial random distribution of elements (with possible overlap) is iteratively modified to minimise the system energy depending on

*Corresponding author, e-mail: marekm@imc.pcz.czest.pl

the degree of overlap between the elements (or the column wall) and potential energy related to their position above the column base (Abreu et al., 2003; Nolan and Kavanagh, 1995; Roskilly et al., 2010). There are also random walk algorithms (Jia and Williams, 2001; Ritvanen and Jalali., 2008) and procedures treating the packing as an optimisation problem (Nandakumar et al., 1999).

The experimental investigations of random packed beds are usually based on Gamma or X-ray tomography and image analysis (Benyahia, 1996; Wang et al., 2001; Zhang et al., 2006). This examination reveals (together with numerical simulation mentioned above) the characteristic porosity distribution inside the bed – an oscillating pattern with maximum value on the container wall and stabilising in the bed interior a few element diameters away from the wall. The comparison of different simulation results with experimental data is presented in (Toit, 2008).

Spatial variation of porosity is essential to the two-phase flow through the bed and leads to so-called *channeling* effect (liquid maldistribution, in particular the concentration near the container wall). In consequence, the porosity profile is of interest for the practitioners but also for scientists dealing with simulations of the flow and chemical reactions in the fixed bed within simplified frameworks based on averaged flow equations.

In this paper, a new method of numerical generation of a random packed bed of equilateral cylinders is presented. It employs a simplified mechanics of the filling process, similar to the one described in (Zhao et al., 2011) but differing in certain aspects with the known models (e.g. denser packing is obtained with the use of additional centrifugal force). The advantage of the method is that its implementation, compared to other approaches, is straightforward.

The final structures for three different container diameters are examined with respect to global porosity and radial distribution of local porosity. The results are compared for the case of purely random packing with low density and the case of denser packing when the artificial centrifugal force is included.

2. GENERATION OF A BED STRUCTURE

The proposed method of the bed structure generation is based on the following assumptions:

- elements are added to the bed in a sequential manner (one by one);
- when an element is inserted into the bed structure its position and orientation remains unchanged to the end of the simulation; this will be further referred to as *frozen bed* assumption;
- initially an element is placed above the bed with random position and orientation;
- an element moves under the action of gravity and reaction forces in case of contact with the bed, the base or the wall of the column (see Fig. 1);
- in a given time step the resultant force exerted on the element leads to translation of its center of mass in the direction of the force vector and the resultant moment – to rotation of the element about the axis defined by the moment vector (in a complete mechanical model the force results in a change of linear velocity, the moment – change of angular velocity, see (Siiria and Yliruusi., 2007)); such simplified mechanics of the process may be understood as a motion in a highly viscous medium;
- the motion of an element is tracked until mechanical equilibrium is reached; in such a case the element becomes a component of the bed (and remains at rest).

It should be emphasised that from the point of view of the purpose of the simulation, which is obtaining the final structure in mechanical equilibrium (at least approximately), simplifications in the mechanics are not significant. Although the frozen bed assumption may lead to locally unstable structures, such cases are relatively rare and should not considerably influence the statistical properties of the bed (as its porosity). On the other hand, the implementation of the model is greatly simplified, if the interaction of

only one element with the fixed structure needs to be analysed. A complete mechanical model requires, in principle, taking into account interactions between all the bed elements (direct or indirect), which is difficult and more time consuming.

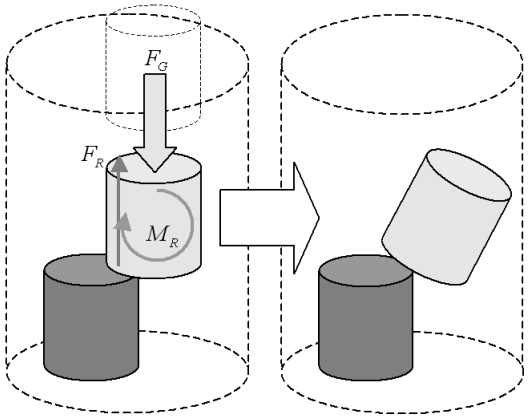

Fig. 1. Forces exerted on the new element – gravity and reactions in case of contact with the bed

As mentioned earlier, for a proper packing algorithm a method is needed for overlap detection between the bed elements. It turns out that for two cylindrical elements defined by the position of their centres, dimensions and spatial orientation (e.g. axial vector), overlap detection is a non-trivial task and requires an intricate geometrical analysis (Kodam et al., 2010) The problem is even more complex for slightly modified shapes like Raschig ring. In the present model this issue is addressed by covering of the element surface with a dense grid of points – markers. The problem of overlap detection for cylinders is then reduced to checking whether any marker on the element surface lies inside the other cylinder, which is trivial and can be performed in the following way.

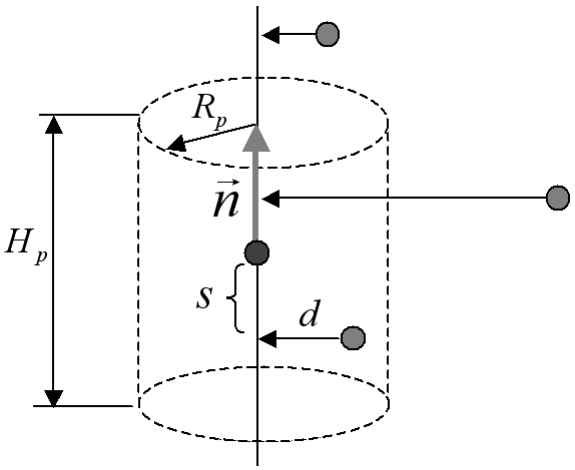

Fig. 2. The bed element and the definition of quantities relevant for collision detection

The given point is projected on the cylinder axis and two quantities are determined: d - distance from the axis, s - distance of the projection from the cylinder centre. The point lies inside the cylinder of radius R_p and height H_p when (see Fig. 2):

$$d < R_p, \quad s < H_p / 2 \tag{1}$$

Moreover, this approach allows for easy calculation of the degree of overlap x which is essential for estimation of reaction forces. For instance, for a marker inside the cylinder, close to its wall, x can be found as:

$$x = R_p - d \tag{2}$$

The number of markers in the grid depends on the expected resolution. The more markers, the more accurate the representation of the cylinder surface. However, the computational load also increases, thus a reasonable compromise between the computational cost and accuracy should be attained. One must be aware that too coarse grid may result in partial overlap between bed elements, especially near the edge of the cylinders. The issue of overlap is analysed in detail further in this section.

In each time step the force $\mathbf{F}_i$ exerted on i-th marker is calculated. This force may be expressed as the sum of gravity force **G** - constant value directed towards the base of the column - and the reaction force $\mathbf{R}_i$:

$$\mathbf{F}_i = \mathbf{G} + \mathbf{R}_i \tag{3}$$

The reaction force is assumed to be proportional to the degree of overlap x_i between the particular marker and the bed element C_b:

$$\mathbf{R}_i = kx_i\mathbf{r} \tag{4}$$

In consequence the marker tends to be pushed away from the bed element and overlap is eventually reduced.

The selection of particular value of the stiffness coefficient depends on the required separation of the bed elements. The higher the stiffness, the smaller overlap of the elements in the state of the equilibrium. However, one should bear in mind that with increasing value of stiffness the time step must be decreasing in order to ensure the stability of calculations. The instability may occur when in a given time step a marker is placed inside some of the bed elements and the force assigned to the marker is so large that the newly added element is rejected far from the present position.

The resultant force **F** and moment **M** exerted on the element is found as a composition of the forces and moments (respectively) acting on the element markers:

$$\mathbf{F} = \sum_i \mathbf{F}_i, \quad \mathbf{M} = \sum_i (\mathbf{r}_i - \mathbf{r}_{pc}) \times \mathbf{F}_i \tag{5}$$

Translation $\Delta\boldsymbol{s}$ and rotation angle $\Delta\varphi$ about the axis appointed by vector **M** is found as:

$$\Delta\mathbf{s} = C_F\mathbf{F}\Delta t, \quad \Delta\varphi = C_M\,|\,\mathbf{M}\,|\,\Delta t \tag{6}$$

When in a given time step the following relations are fulfilled:

$$|\,\Delta\mathbf{s}\,| < \varepsilon_s, \quad |\Delta\varphi| < \varepsilon_\varphi \tag{7}$$

i.e. magnitudes of translation and rotation considered as close to zero (the criterion of mechanical equilibrium), the motion of the given element is no longer tracked and the element is inserted into the bed structure.

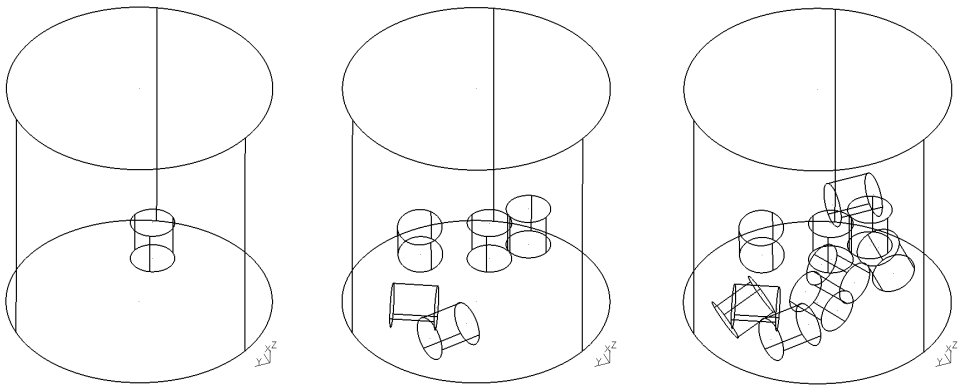

Fig. 3. Consecutive stages of the bed generation (1, 5 and 10 cylinders, respectively)

An example process of the bed generation within a cylindrical container is shown in Fig. 3 (three stages with 1, 5 and 10 bed elements, respectively).

As will be demonstrated in the next section, the described method leads to rather loose packing of the elements. This is the consequence of purely random deposition of the cylinders and frozen bed assumption. Too increase the packing density another force can be included in the model. The additional force $\mathbf{F}_{CF}$ acts in each marker in the direction perpendicular to the container axis towards the column wall (it can be interpreted as centrifugal force but does not depend on the distance from the container axis). Thus, instead of (3), we have:

$$\mathbf{F}_i = \mathbf{G} + \mathbf{R}_i + \mathbf{F}_{CF,i} \tag{8}$$

The addition of anew element to the bed is divided into three stages: 1) free fall ($\mathbf{F}_{CF} = 0$) , 2) action of the centrifugal force (at this stage the element is pressed against the container wall or other bed elements), 3) another stage of free fall ($\mathbf{F}_{CF} = 0$). The last stage is added to ensure that the artificial force does not influence the final state of mechanical equilibrium.

This modification of the algorithm results in much denser packing structures resembling the ones obtained in experiments. In Fig. 4 such a structure is presented for a bed containing about 4000 elements. Despite the probabilistic nature of the procedure partial ordering of the elements may be noticed on the container base and the wall, which is in good agreement with literature data (Zhang et al., 2006). The ordering results in characteristic pattern of porosity profiles examined in the next section.

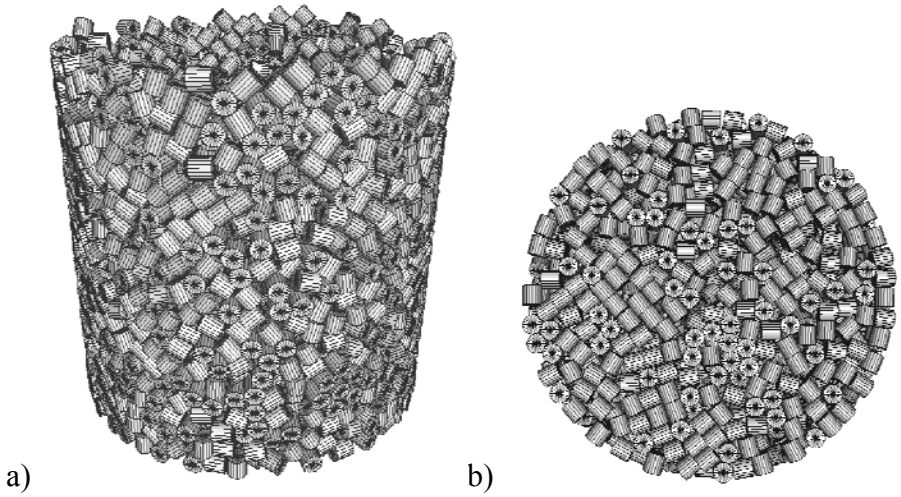

a) b)

Fig. 4. Sample bed structure generated with the described algorithm (a) and view from the bottom (b). The container wall is not shown for clarity

The overlap between the elements has been studied in the case of a bed consisting of 1500 elements for two different numbers of markers covering the element surface (750 and 6000). The calculation of overlap was performed as follows. After each simulation step, when a particular element was added to the bed, a very dense regular grid of points was distributed on the element's surface (750000 points). The grid can be considered as an accurate representation of the element's surface and is used only for calculation of overlap (not for the element's motion). For each point the normalised degree of overlap was found as: x/D_p where x is taken as 0 for the points not immersed in any element. For a given element the overlap was defined as the maximum value taken over all of the element's points. The probability distribution of overlap is shown in Fig. 5. In the case of 750 markers, the average overlap is about 2.5% of the element diameter with values below 5% dominating in the considered bed (however, values as high as 9% are reached for some of the elements). When 6000 markers are used, the average

overlap is about 1% with the maximum value about 3%, which is quite satisfactory, although the simulation time is almost three times longer. Depending on the required accuracy and the quality of the bed geometry, the number of markers may be increased at the cost of computational time. It can be remarked that generation of the bed shown in Fig. 4 (4000 elements, 750 markers) takes about 8 hours on a typical desktop PC (AMD Athlon, 2.21 GHz). However, no special effort has been made to optimise the computer code implementing the proposed method and significant reduction of computational time may be expected when more efficient data structures are used.

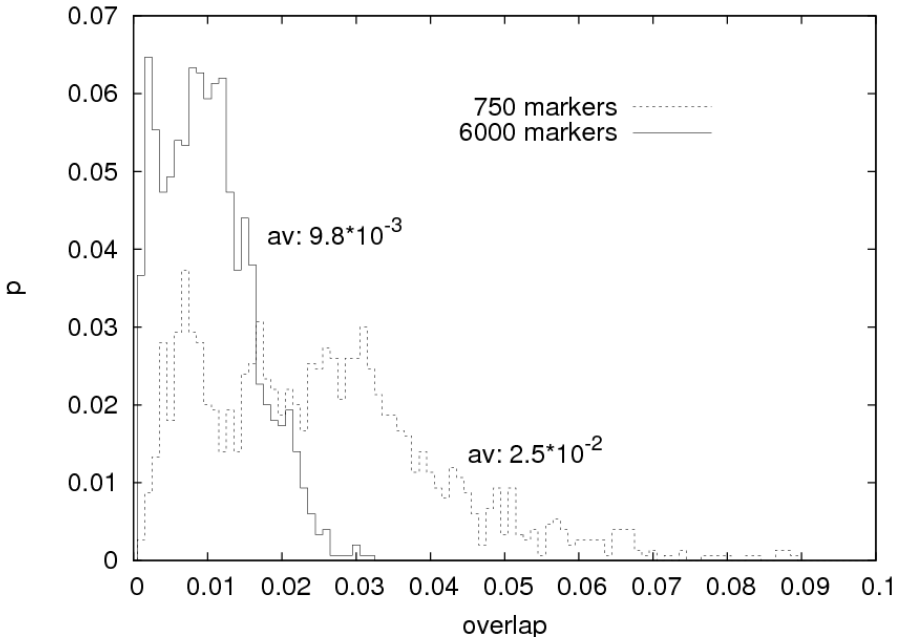

Fig. 5. Probability distribution of overlap for two different numbers of markers and average value of overlap for the two cases

The remaining part of this paper is devoted to analysis of the structures obtained for different container diameters (keeping unit size of the elements, $D_p = H_p = 1$). The role of centrifugal force is also investigated. The six considered test cases are described in Tab. 1 (D_c - container diameter).

Table 1. Definition of the test cases

Case	C1	C2	C3	C4	C5	C6
F_{CF}	0	0	0	1.0	1.0	1.0
D_c / D_p	10	15	20	10	15	20

The following values of model parameters are selected: $|\mathbf{G}| = 1.0$, $k = 10^2$, $\Delta t = 10^{-3}$, $\varepsilon_s = \varepsilon_\varphi = 10^{-5}$, 750 markers per element (distributed uniformly over the surface), $C_F = C_M = 1.0$. The filling process is stopped when a single element reaches the height of $20D_p$.

3. POROSITY CALCULATIONS

3.1. Global porosity

The global porosity coefficient ε, sometimes termed also as *void fraction*, is defined as the ratio of the

empty space volume V_{void}, space between the bed elements, to the total considered bed volume V_{tot}:

$$\varepsilon = \frac{V_{void}}{V_{tot}} \tag{9}$$

The procedure for calculation of ε may be as follows. A plane perpendicular to the container axis is introduced at the height h above the column base. The volume of the bed below the plane is taken as V_{tot}:

$$V_{tot} = \pi R_c^2 h \tag{10}$$

However, the exact calculation of V_{void} in this case is a complicated geometrical task, as the plane, in general, cuts the bed through the cylindrical elements and volume of different sections of cylinder should be known. For triangulated elements the procedure described in (Nandakumar et al., 1999) may be employed. This complication can be avoided by calculating V_{void} as:

$$V_{void} = V_{tot} - N(h)V_p \tag{11}$$

where $N(h)$ is the number of elements whose centres are below the plane. Of course, the method introduces en error which magnitude depends on the relation between the total volume and volume cut from the cylinders near the plane. This error can be made statistically irrelevant taking sufficiently large plane height h. Using (11) the porosity is found as:

$$\varepsilon(h) = 1 - N(h)\left(\frac{R_p}{R_c}\right)^2 \frac{H_p}{h} \tag{12}$$

This method has been used for estimation of porosity for the packed beds generated with the algorithm presented in Section 2. As shown in Fig. 6 (test cases C1 and C4) the value of ε indeed stabilises when h is large enough. The increase at the end of the considered range is caused by the specific structure at the upper part of the bed: pile for purely random deposition and funnel in case of centrifugal force. For other test cases the graphs are very similar, thus they are not included. It can be seen that simulations with centrifugal force lead to structures of considerably smaller porosity (decrease from 0.479 to 0.387 for C1 and C4).

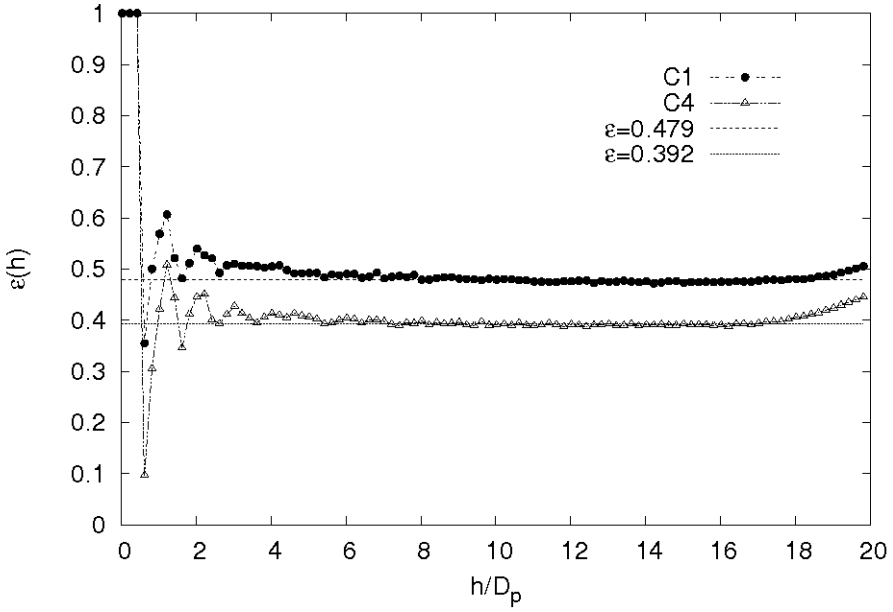

Fig. 6. The dependence of the calculated global porosity on the selected height h (cases C1 and C4). The horizontal lines correspond to the values of porosity calculated with MC method

The method defined by (12), further referred to as *geometrical*, obviously is suitable only for estimation of global porosity. When local variations of porosity are of interest much smaller sample volume should be taken and the simplified approach fails. To deal with this problem, another method – Monte Carlo (MC) – has been considered in which a large number of points (~10^6) is randomly distributed in the sample volume and the porosity is estimated by the ratio of number of points placed in the empty space to the total number of points. Such methodology can be employed regardless of the sample volume size – for global and local porosity estimations (see subsection 3.2). In Tab. 2 the results obtained with both methods – geometrical and MC – are compared for all test cases. Generally, MC slightly overestimates the bed porosity.

Table 2. Global porosity for different test cases obtained with geometrical and Monte Carlo method

Case	C1	C2	C3	C4	C5	C6
ε (geom.)	0.479	0.466	0.459	0.387	0.386	0.386
ε (MC)	0.479	0.472	0.466	0.392	0.390	0.389

3.2. Radial porosity profile

For some applications global porosity coefficient, characterising the bed as a whole, does not deliver enough information about the bed structure. Distribution of porosity within a bed may be highly non-uniform and structures of the same global porosity could behave completely different e.g. with respect to flow conditions. However, one should be careful dealing with local porosities, as the results strongly depend on the size of sample volumes and their definition.

In the present work the radial distribution of porosity has been examined for numerically generated packed beds (cases C1-6). The sample volume in this case is defined as an annular ring of width equal $0.1D_p$, coaxial with the container and of height equal $10D_p$. MC method has been employed to estimate the local porosity ε_{loc} of the ring. The results are presented in Fig. 7-9. The distribution of local porosity is expressed in terms of normalised distance ξ from the container wall (Zhang et al., 2006):

$$\xi = \frac{R_c - r}{D_p} \tag{13}$$

where r- radius of the annular ring comprising the sample volume.

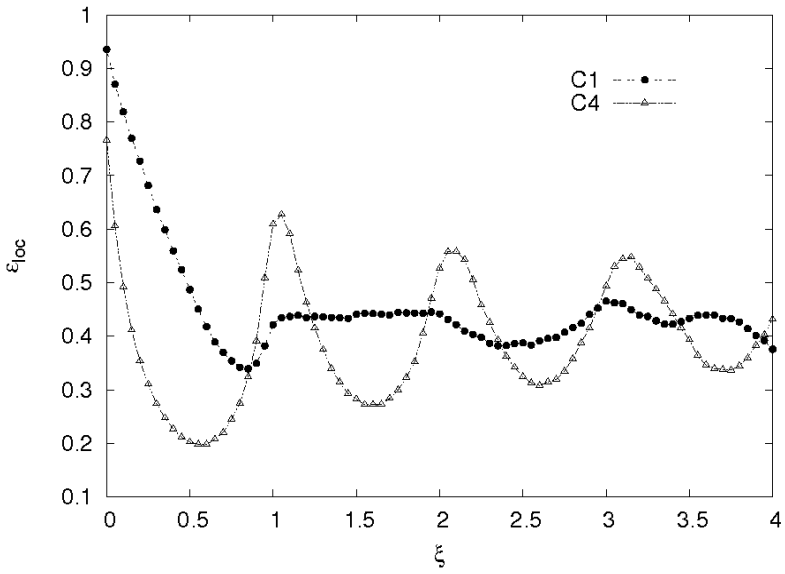

Fig. 7. Radial porosity profile (cases C1 and C4)

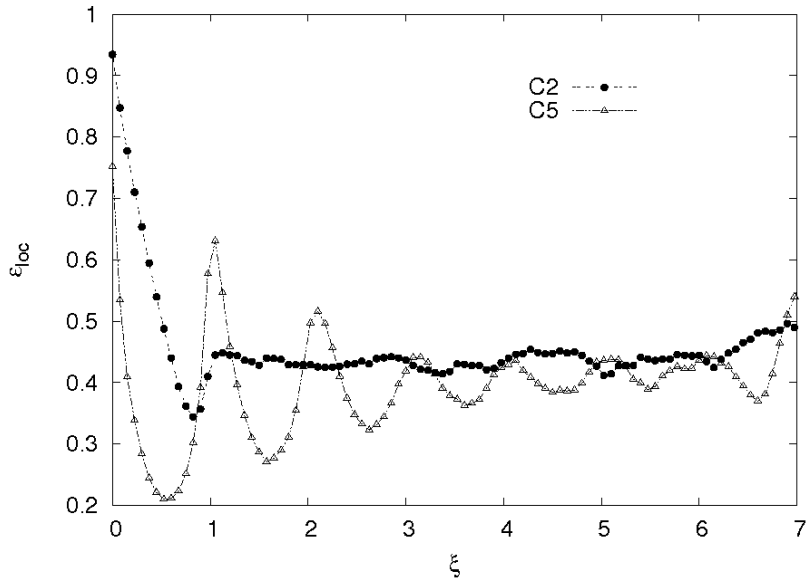

Fig. 8. Radial porosity profile (cases C2 and C5)

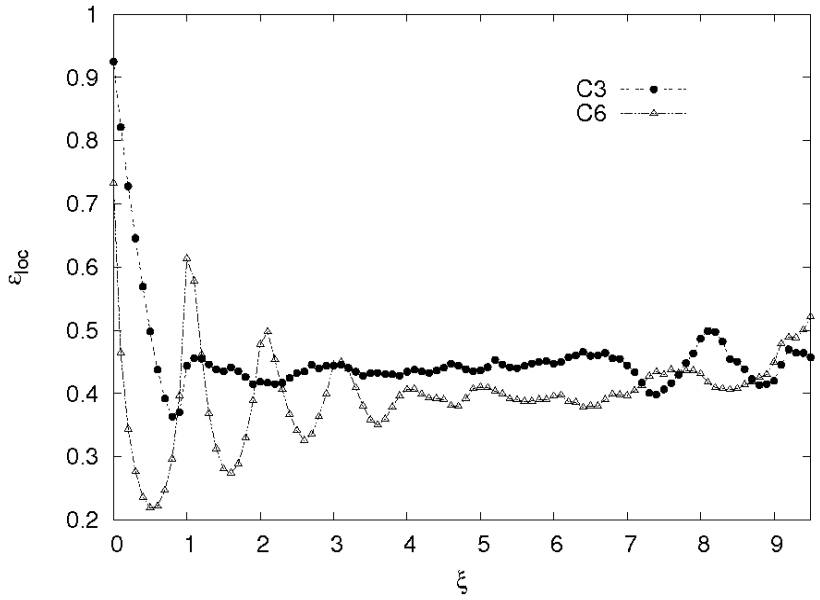

Fig. 9. Radial porosity profile (cases C3 and C6)

It can be seen that in all test cases the porosity markedly increases near the container wall, up to 1.0, depending on the width of the sample volume. However, the inclusion of centrifugal force and denser packing of the elements result in oscillating profile of local porosity. The profiles can be directly connected with partial ordering of the bed elements, as shown in Fig. 10. Distribution of element centres is nearly uniform for loose packing (cases C1-3) and reveals characteristic oscillating pattern for denser packing (cases C4-6). The partial ordering reaches up to 4-5 element diameters into the column interior and is especially relevant for columns of smaller diameters. When $D_c \gg D_p$ the elements in interior of the bed can be considered as disordered, similarly to the loose packing case.

The character of porosity oscillations agrees reasonably well with the experimental data. In Fig. 10 comparison with data of (Zhang et al., 2006) is shown for minimum and maximum density packing of cylinders (E1 and E2, respectively). Quantitative comparison with experimental data of (Giese et al., 1998) reveals good agreement near the container wall but, as the spatial scale of the oscillations is a little larger in the numerical simulation, discrepancies arise in the bed interior (Fig. 11).

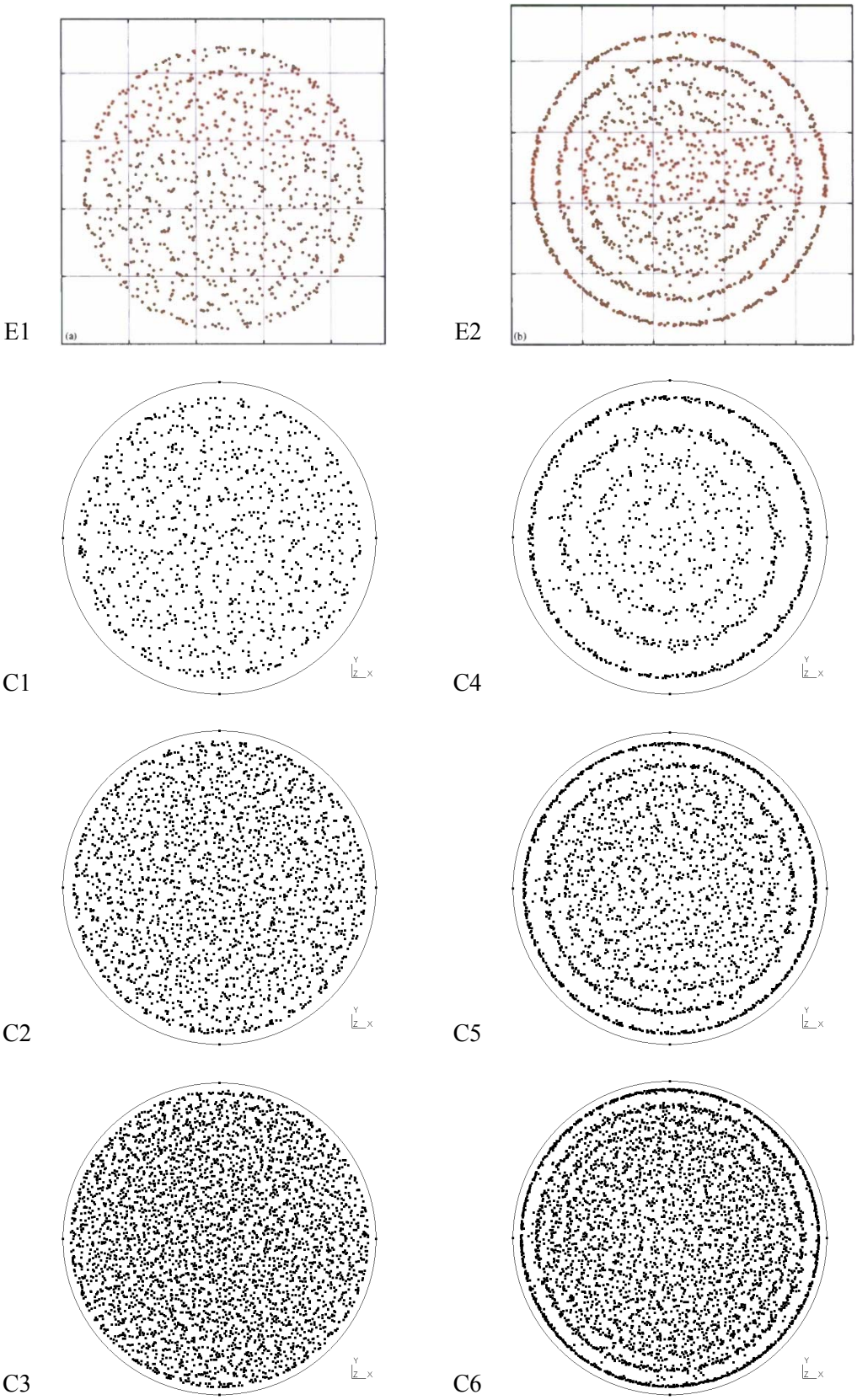

Fig. 10. Distribution of element centres (view from the top). Cases E1 and E2 correspond to the experimental data of (Zhang et al., 2006), minimum and maximum density packing, respectively (reprinted with permission from Elsevier)

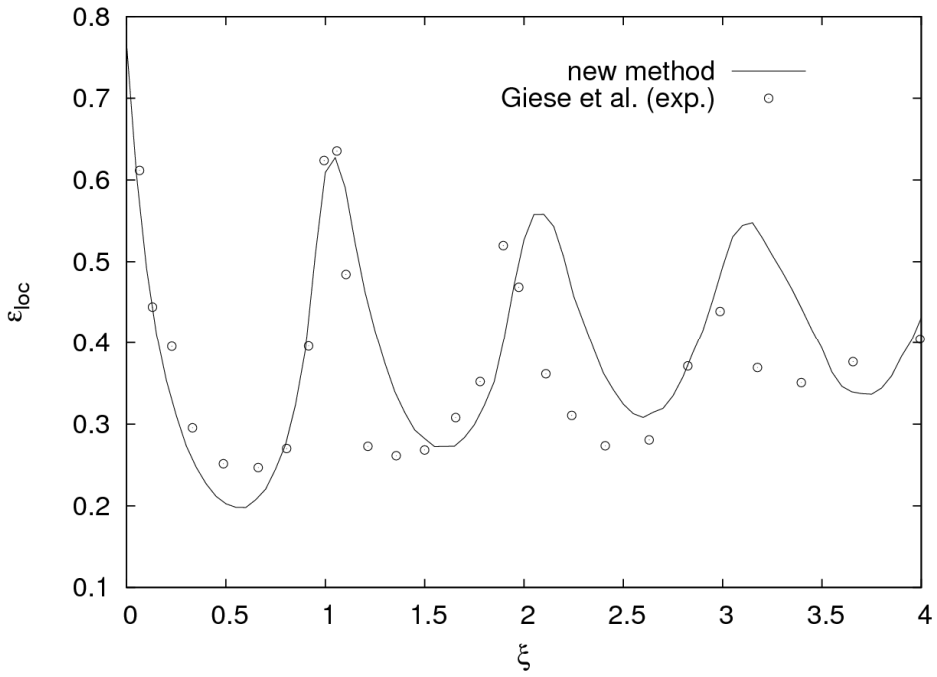

Fig. 11. Radial porosity profile - quantitative comparison with experimental data of Giese et al. (1998)

4. CONCLUSIONS

- A new method has been presented for numerical generation of a fixed random packed bed; the method is based on simplified mechanics of the filling process; the implementation of the method is straightforward compared to other models.
- Elements are added in a sequential manner; motion of an element is analysed until it reaches mechanical equilibrium; denser packing of the elements is achieved by inclusion of artificial centrifugal force.
- Distribution of porosity has been calculated; the radial profiles display the oscillating behaviour known from the literature; the character of the profile is a consequence of partial ordering of the bed elements
- It should be noted that the proposed method may easily be adopted for bed elements of slightly more complex shapes e.g. Raschig rings, for which detection of overlap with a single point is also straightforward; this will be covered in future work.

The work supported by Strategic Research Programme nr SP/E/1/67484/10.

SYMBOLS

C_b	bed element
C_F	model constant (for translation), s/kg
C_M	model constant (for rotation), s/kg
d	distance of the point from the element axis, m
D_c	column diameter, m
D_p	element diameter, m
F	resultant force, N

$\mathbf{F}_i$	force exerted on *i*-th marker, N
$\mathbf{F}_{CF}$	artificial centrifugal force, N
$\mathbf{G}$	gravity force, N
H_p	element height, m
h	height of the cutting plane, m
k	stiffness coefficient, N/m
$\mathbf{M}$	resultant moment, Nm
$N(h)$	number of bed elements below the cutting plane
R_c	column radius, m
R_p	element radius, m
$\mathbf{R}_i$	reaction force exerted on *i*-th marker, N
$\mathbf{r}$	radial vector, m
$\mathbf{r}_i$	position vector of *i*-th marker, m
$\mathbf{r}_{pc}$	position vector of the element center, m
r	radius of the annular ring (sample volume), m
s	distance of the point projection from the element center, m
V_{void}	void volume below the cutting plane, m^3
V_{tot}	total volume below the cutting plane, $[m^3$
x	degree of elements overlap, m

Greek symbols

$\Delta\varphi$	angle of element rotation in a given time step, rad
Δs	element translation in a given time step, m
Δt	time step, s
ε	global porosity coefficient
ε_{loc}	local porosity coefficient
ε_φ	equilibrium criterion for rotation, rad
ε_s	equilibrium criterion for translation, m
ξ	normalised distance from the column wall

Subscripts

c	denotes the column (container)
p	denotes the bed element (particle)
i	denotes *i*-th marker

REFERENCES

Abreu C.R.A, Tavares F.W., Castier M., 2003. Influence of particle shape on the packing and on the segregation of spherocylinders via Monte Carlo simulations. *Powder Technol.*, 134, 167-180. DOI: 10.1016/S0032-5910(03)00151-7.

Benyahia F., 1996. On the global and local structural properties of packed beds on nonequilatelar cylindrical particles. *Particul. Sci. Technol.*, 14, 221-237. DOI: 10.1080/02726359608906697.

Caulkin R., Ahmad A., Fairweather M., Jia X., Williams R. A., 2009. Digital predictions of complex cylinder packed columns. *Comput. Chem. Eng.*, 33, 10-21. DOI: 10.1016/j.compchemeng.2008.06.001.

Jia X., Williams R. A., 2001. A packing algorithm for particles of arbitrary shapes. *Powder Technol.*, 120, 175-186. DOI: 10.1016/S0032-5910(01)00268-6.

Giese M., Rottschafer K., Vortmeyer D., 1998. Measured and modeled superficial flow profiles in packed beds with liquid flow. *AIChE J.*, 44, 484-490. DOI: 10.1002/aic.690440225.

Guo Y., Wassgren C., Ketterhagen W., Hancock B., Curtis J., 2012. Some computational considerations associated with discrete element modeling of cylindrical particles. *Powder Technol.*, 228, 193-198. DOI: 10.1016/j.powtec.2012.05.015.

Kodam M., Bharadwaj R., Curtis J., Hancock B., Wassgren C. A., 2010. Cylindrical object contact detection for use in discrete element method simulations. Part I – Contact detection algorithms. *Chem. Eng. Sci*., 65, 5852-2862. DOI: 10.1016/j.ces.2010.08.006.

Matuttis H.G., Luding S., Herrmann H.J, 2000. Discrete element simulations of dense packings and heaps made of spherical and non-spherical particles. *Powder Technol*., 109, 278-292. DOI: 10.1016/S0032-5910(99)00243-0.

Mueller G.E., 2005. Numerically packing spheres in cylinders. *Powder Technol*., 159, 105-110. DOI: 10.1016/j.powtec.2005.06.002.

Mueller G.E., 1992. Radial void fraction distributions in randomly packed fixed beds of uniformly sized spheres in cylindrical containers. *Powder Technol*., 72, 269-275. DOI: 10.1016/0032-5910(92)80045-X.

Nandakumar K., Yiqiang S., Chuang K.T., 1999. Predicting geometrical properties of random packed beds from computer simulation. *AIChE J*., 45, 2286- 2297. DOI: 10.1002/aic.690451104.

Nolan G.T., Kavanagh P.E., 1995. Random packing of nonspherical particles. *Powder Technol*., 84, 199-205. DOI: 10.1016/0032-5910(95)98237-S.

Ritvanen J., Jalali P., 2008. On near-wall effects in hard disk packing between two concentric cylinders. Physica A., 387, 5381–5386. DOI: 10.1016/j.physa.2008.05.035.

Roskilly S.J., Colbourn E.A., Alli O., Williams D., Paul K. A., Welfare E.H., Trusty P.A., 2010. Investigating the effect of shape on particle segregation using a Monte Carlo simulation. *Powder Technol*., 203, 211-222. DOI: 10.1016/j.powtec.2010.05.011.

Salvat W.I., Mariani N.J., Baretto G.F., Martinez O.M., 2005. An algorithm to simulate packing structure in cylindrical containers. *Catal. Today*., 107, 513-519. DOI: 10.1016/j.cattod.2005.07.108.

Siiria S., Yliruusi J., 2007. Particle packing simulations based on Newtonian mechanics. *Powder Technol*., 174, 82-92. DOI: 10.1016/j.powtec.2007.01.001.

Theuerkauf J., Witt P., Alli O., Schwesig D., 2006. Analysis of particle porosity distribution in fixed beds using the discrete element method. *Powder Technol*., 165, 92-99. DOI: 10.1016/j.powtec.2006.03.022.

Toit C.G., 2008. Radial variation in porosity in annular packed beds. *Nucl. Eng. Des.*, 238, 3073-3079. DOI: 10.1016/j.nucengdes.2007.12.018.

Wang Z., Afacan A., Nandakumar K., Chuang K.T., 2001. Porosity distribution in random packed columns by gamma ray tomography. *Chem. Eng. Process.*, 40, 209-219. DOI: 10.1016/S0255-2701(00)00108-2.

Zhang W., Thompson K., Reed A.H., Beenken L., 2006. Relationship between packing structure and porosity in fixed beds of equilateral cylindrical elements. *Chem. Eng. Sci.*, 61, 8060-8074. DOI: 10.1016/j.ces.2006.09.036.

Zhao J., Li S., Lu P., Meng L., Li T., Zhu H., Shape influences on the packing density of frustums. *Powder Technol*. 2011, 214, 500-505. DOI: 10.1016/j.powtec.2011.09.013.

Received 13 November 2012
Received in revised form 23 May 2013
Accepted 30 May 2013